

Magnetic structure of deformation-induced shear bands in amorphous $\text{Fe}_{80}\text{B}_{16}\text{Si}_4$ observed by magnetic force microscopy

G. W. Brown^{a)}

Center for Materials Science, Los Alamos National Laboratory, Los Alamos, New Mexico 87545

M. E. Hawley

Materials Science and Technology Division, (MST-8), Los Alamos National Laboratory, Los Alamos, New Mexico 87545

D. J. Markiewicz

Department of Chemistry, Princeton University, Princeton, New Jersey 08544

F. Spaepen and E. P. Barth

Division of Engineering and Applied Sciences, Harvard University, Cambridge, Massachusetts 02138

Processing-induced magnetic structures in amorphous metallic alloys are of interest because of their impact on the performance of materials used in electric device applications. Plastic deformation associated with cutting or bending the material to the desired shape occurs through the formation of shear bands. The stress associated with these shear bands induces magnetic domains that can lead to power losses through interaction with the fields and currents involved in normal device operation. These domains have been studied previously using a variety of techniques capable of imaging magnetic domain structures. In an effort to better characterize and understand these issues, we have applied atomic and magnetic force microscopy to these materials to provide three-dimensional nanometer-scale topographic resolution and micrometer-scale magnetic resolution. © 1999 American Institute of Physics. [S0021-8979(99)76508-4]

INTRODUCTION

Plastic deformation in amorphous materials, induced by cutting or bending the material to the desired shape, often occurs through formation of shear bands,¹ which are analogous to slip bands in crystalline materials. In electric power applications it is important to characterize and understand the properties of the magnetic structures induced by these shear bands. Our interest here is to exploit the power of atomic and magnetic force microscopy (MFM) towards these goals. MFM is an extension of atomic force microscopy (AFM), which uses a traditional AFM tip coated with magnetic material to sense the magnetic structure at a surface with ~ 20 nm ultimate resolution.

MAGNETIC STRUCTURE

A material's magnetic structure is determined by the configuration of spins which minimizes the total magnetic energy. In deformed, amorphous melt-spun ribbons, without external fields, this includes contributions from shape and stress anisotropies, and magnetostatic and magnetic exchange effects. The anisotropies determine the easy magnetization direction and the final magnetic structure is a compromise between shape anisotropy aligning the magnetization (\mathbf{M}) with the longest axis, stress anisotropy aligning \mathbf{M} along the direction of largest stress, and demagnetizing effects breaking large domains into smaller ones and setting up closure domains to contain the flux. Domain structures will be discussed below. Shape anisotropy effects can

be large due to the high aspect ratio of melt-spun ribbons. Rapid quenching and process-induced stress anisotropy can have the strongest effect, manifested through the magnetoelastic energy (ME),

$$E_{\text{ME}} = -\frac{3}{2} \lambda \sum_{i=1}^3 \sigma_i \gamma_i^2, \quad (1)$$

to the lowest order, where λ is the material-dependent magnetostriction constant and the γ_i 's are the direction cosines of \mathbf{M} with respect to the principal stress axes. For positive λ materials, such as FeBSi alloys, \mathbf{M} will align along the direction of most positive (or least negative) stress. In plastic deformation, the final stress state is a superposition of the stress due to the damage structures with residual stress, which occurs on unloading.

Domain formation minimizes the net magnetization by breaking it up into smaller domains having different orientations (demagnetization) and closure domains keeping flux within the material. Demagnetization segregates spins into oppositely aligned domains separated by 180° domain walls. These fine domains have a net overall attraction for each other and lower the total energy. They also satisfy the magnetoelastic energy since they point along (parallel or antiparallel to) the easy axis. Any excessive stray field flux is reduced by in-plane closure domains, separated from the vertical domains by 90° walls.

The actual observed domain structure is often complicated by defects, microstructure, and the material's previous exposure to fields. In general, increasing the number of domains lowers the total energy. However, smaller domains mean more domain walls. Despite these complications, con-

^{a)}Electronic mail: geoffb@lanl.gov

clusions can be drawn from MFM data since they reproduce general features of stress-induced domain structures observed and understood from previous experiments by Livingston and co-workers²⁻⁵ using Bitter-pattern optical and Lorentz-force scanning electron microscopies. For in-plane magnetization, the general trend is for the domains to segregate into bands of alternating orientation in the surface direction normal to the easy axis. For out-of-plane magnetization, the magnetization breaks into bands, but meanders in the surface plane unless some other aspect influences its direction. In-plane closure domains also form and sometimes acquire a zigzag boundary structure. Explanation of zigzags arising from head-to-head domains such as these include rapidly alternating oblique orientation of the walls' surface projection² and energy gained by lengthening the wall and spreading out the magnetic pole distribution the head-to-head region approximates.⁶⁻⁸

PREVIOUS RESULTS ON FeBSi MATERIALS

Lakshmanan and co-workers⁹⁻¹¹ have used Bitter-pattern optical microscopy to examine the shear-band-induced magnetic structure in $\text{Fe}_{78}\text{B}_{13}\text{Si}_9$. From two-dimensional optical data on the tensile side of the bending, they observed fine, zigzag closure domains normal to the shear step edges. These domains decreased in intensity farther from the shear step, gained components parallel to step edges farther from the step, and were ~ 3 times longer on the elevated side of the shear steps as compared to the lower side. These features persisted after the steps were electropolished away, indicating that the magnetic structure arose from subsurface stress associated with the shear band. On the compressive side of the bending, the domain patterns were described as straight 180° domain walls separating in-plane domains oriented at 90° to the shear steps. These patterns did not persist upon electropolishing. Instead, a thin collection of colloid at the shear step was observed, indicating a stress-induced in-plane anisotropy on both sides of the step, but that the step itself was necessary to nucleate the domains and induce demagnetization energy.

From the magnetic data, Lakshmanan and co-workers inferred compressive and tensile side "dislocation array" structures. These qualitatively account for the topography and magnetic structure that they observed in their optical experiments but the concept of a dislocation in amorphous material is not defined. However, knowing the displacement, the concept of a dislocation core can be useful in a continuum model to calculate stresses associated with shear bands and compare to observed magnetic structure.

EXPERIMENT

We examined $\text{Fe}_{80}\text{B}_{16}\text{Si}_4$ ribbons¹² which were plastically deformed by uniaxially bending them between platens. For tensile side studies, residual bend angles of between 60° and 103° were examined. For compressive side studies, low ($<20^\circ$) residual angles were examined. In every case, the smooth face (opposite the melt-spin wheel in fabrication)

was used. The samples were ultrasonically cleaned in methanol and dried in flowing nitrogen before AFM/MFM investigation.

MFM data were acquired in a noncontact, dual-pass "lift-mode"¹³ technique with commercially available, $225 \mu\text{m}$ long CoCr-coated Si MFM tips on Si cantilevers having resonant frequencies from 50 to 70 kHz. The dual-pass technique provides three-dimensional topographic data and corresponding magnetic structure data with minimal crosstalk. All tips were poled perpendicular to the surface of the material and were, therefore, sensitive to stray field gradients from z -oriented domains or the z components of domains oblique to the surface. No effect of tip polarization magnitude was seen on the sample domain structure.

RESULTS AND DISCUSSION

Tensile and compressive sides exhibit up and down shear steps on either side of the bend center. Figure 1 shows a typical example of AFM/MFM data for each side with line sections illustrating step profiles in greater detail. A previously unreported interesting physical feature of the terraces is their curvature, which we verified by imaging with non-magnetic tips in tapping and contact modes. The curvature of a terrace depends on the nature of the steps bounding it. Positive curvature (second derivative of the surface outline >0) is observed for plateaus. Negative curvature is observed for valleys. When a terrace is bounded by an up step on one side and a down step on the other, the curvature is positive for a compressive side terrace and varies from positive (top of the step) to negative (bottom of the step) for a tensile side

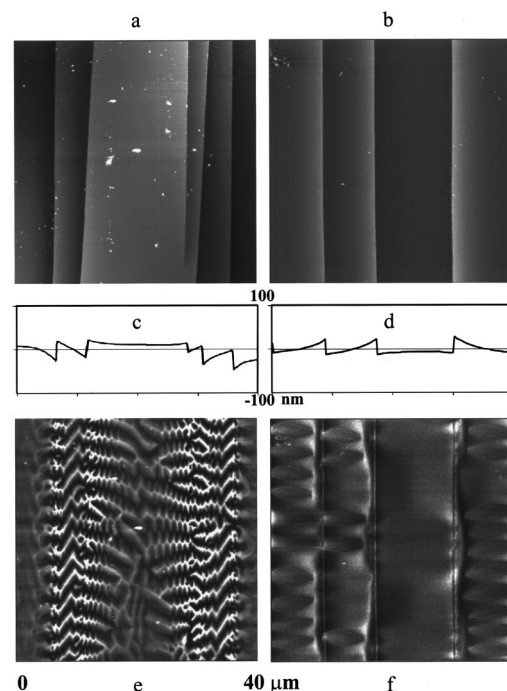


FIG. 1. Topographic images in plan view of the tensile (a) and compressive (b) sides of bent amorphous ribbons. Corresponding line scans (c) and (d) are shown for each to show the profiles in better detail. At the bottom (e) and (f) are the corresponding magnetic structures.

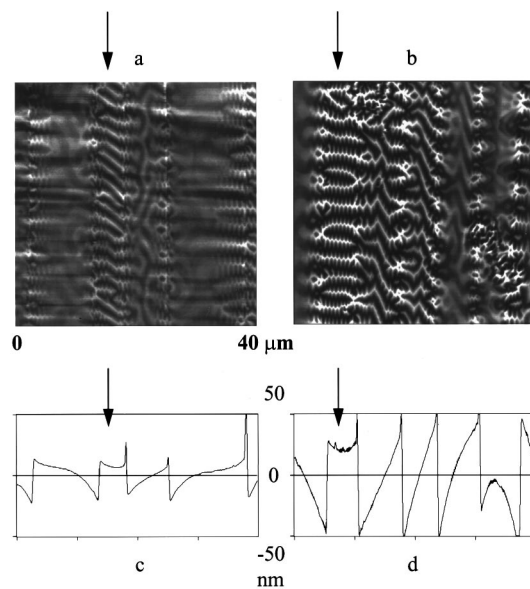


FIG. 2. MFM images of the magnetic structure for two ribbons with different residual bend angles. The arrows highlight up-down steps with the same shear bandwidth, $\sim 5 \mu\text{m}$, but different height. The first is about half the height of the second, which is reflected in the significantly different magnetic structure and out-of-plane intensity. In image (b), the zigzag region at either step edge is relatively short and connected by walls at an angle deviating from the perpendicular to the steps.

terrace. To our knowledge, this curvature has not been observed before and is an important clue to understanding how these materials deform and relax.

The corresponding magnetic structure is also shown in Fig. 1. *The tensile side:* Near the tops of the shear steps, the general domain structure is banded along the width of the ribbon with a small-angle zigzag structure and the strongest MFM signal. As these propagate across the terrace, the zigzags diminish, may condense into a fewer number of domains, and often deviate from the step edge perpendicular. At the bottom of a shear step, the MFM signal is weaker and the domains begin to acquire components parallel to the shear steps, in some cases forming loops. Zigzag structures are occasionally observed here but they rarely extend far from the step. Between the shear steps, the MFM signal weakens and the magnetic structure becomes a convolution of the above descriptions. On a narrow terrace with two shear step tops, the banding and zigzag structure can propagate all the way across. Alternatively, for a terrace bounded by a top edge on one side and a bottom edge on the other, the general domain structures meet in the middle and coalesce.

The compressive side: The most regular magnetic feature on the compressive side is the straight line parallel to (and coincident with) the step edges. The rest of the magnetic structure can be classified as “banded” and oriented roughly perpendicular to the step edges, but the domain walls are curved and the width of the domain and curvature of the walls change with the distance from the step. The features are sometimes continuous across the step edges unlike those on the tensile side of the bending. These features are reminiscent of “lozenge” domains,¹⁴ which may provide a clue to the forces behind their structure.

Figure 2 illustrates the dependence of the magnetic

structure on the step height. Here, two virtually identical $5 \mu\text{m}$ wide terraces, bounded by top and bottom step edges, are shown. The step in the left panel is 27 nm high compared to the 65 nm step in the other. The corresponding MFM images show that the taller terrace has a finer domain structure that exhibits both banding and zigzag walls. The shorter terrace only shows banding at the edge with much weaker, shorter zigzag regions, which seems consistent with a lower stress state. Since the step heights depend on the bend angles, an indirect correlation with this can be inferred. While the shear band widths show little or no correlation with the bend angle, the increase in angle is reflected in increasing average shear step height. Assuming increased residual stress with the bend angle, one would expect that to be manifested in the observed magnetic structure.

Based on Livingston’s results, on the tensile side of the bending we seem to be observing a structure consistent with tensile stress along the surface normal and/or in-plane compressive stress. The features we observe appear to be z -oriented domains with in-plane closure domains acquiring a zigzag structure due to their head-to-head orientation. On the compressive side of the bending, our features are consistent with in-plane domains, which implies in-plane tension and/or out-of-plane compression. These are the same stress states inferred by Lakshmanan and co-workers and qualitatively accounted for by the same authors’ dislocation array model. However, it is not clear how their assumed dislocation array accounts for the additional detail observed in our experiments, including the relative step heights and surface curvatures. Their results also do not obviously account for the in-plane magnetization components developed farther from the tops of the step edges. Fortunately, these details provide extra constraints for modeling the deformation and its corresponding magnetic structure so that a consistent view of the microscopic structure can be developed. We are currently exploring these issues in order to obtain a more accurate understanding.

¹F. Spaepen and A. I. Taub, in *Amorphous Metallic Alloys*, edited by F. E. Luborsky (Butterworths, London, 1983), pp. 231–256.

²J. D. Livingston, *Phys. Status Solidi A* **56**, 637 (1979).

³J. D. Livingston and W. G. Morris, *IEEE Trans. Magn.* **MAG17**, 2624 (1981).

⁴J. D. Livingston, W. G. Morris, and F. E. Luborsky, *J. Appl. Phys.* **53**, 7837 (1982).

⁵J. D. Livingston and W. G. Morris, *J. Appl. Phys.* **57**, 3555 (1985).

⁶N. Curland and D. E. Speliotis, *J. Appl. Phys.* **41**, 1099 (1970).

⁷M. J. Freiser, *IBM J. Res. Dev.* **23**, 330 (1979).

⁸X. Y. Zhang, H. Suhl, and P. K. George, *J. Appl. Phys.* **63**, 3257 (1988).

⁹V. Lakshmanan and J. C. M. Li, *Mater. Sci. Eng.* **98**, 483 (1988).

¹⁰V. Lakshmanan, J. C. M. Li, and C. L. Tsai, *Acta Metall. Mater.* **38**, 625 (1990).

¹¹V. Lakshmanan and J. C. M. Li, *J. Mater. Res.* **6**, 371 (1991).

¹²Allied Signal Corp.

¹³Digital Instruments Corp, Santa Barbara, CA.

¹⁴M. Labrune, S. Hamzaoui, C. Battarel, I. B. Puchalska, and A. Hubert, *J. Magn. Magn. Mater.* **44**, 195 (1984).